PERGAMON

International Journal of Multiphase Flow 29 (2003) 329–338

International Journal of Multiphase Flow

www.elsevier.com/locate/ijmulflow

Brief communication

Concentration profiles of droplets and prediction of the transition from stratified to annular flow in horizontal pipes

S. Baik, T.J. Hanratty *

205 Roger Adams Laboratory, Department of Chemical Engineering, University of Illinois at Urban-Champaign, Box C-3, 600 South Mathews Avenue, Urbana, IL 61801, USA

Received 10 July 2002; received in revised form 6 October 2002

1. Introduction

Gravity causes an asymmetric distribution of droplets in the gas phase and of the film flowing along the wall in horizontal annular flows. A knowledge of the concentration profile is needed to predict the rate of deposition. Entrainment is smaller in horizontal flows than in vertical flows because gravity enhances deposition. This effect increases with increasing asymmetry. Unfortunately, the number of studies of droplet distribution is small. These include measurements for air and water flowing in a 5.08 cm pipe (Paras and Karabelas, 1991) and in a 9.53 cm pipe (Williams et al., 1996). The experiments by Dykhno et al. (1994) of secondary velocity fields in horizontal annular flow also include results of some relevance. These studies show that concentration profiles in a direction perpendicular to the gravitational vector are flat over most of the pipe cross section. This approximation is poorer under conditions where secondary flows are important.

Pan and Hanratty (2002) explored a correlation, for the concentration variation in the direction of gravity, wherein gravitational settling is balanced by turbulent diffusion, as suggested by Paras and Karabelas (1991). A correlation, which includes no effect of pipe diameter, was used to predict drop size. The turbulent diffusivity was assumed to be proportional to the product of the diameter of the pipe and the friction velocity. This approach was unsuccessful in relating the experimental results in 5.08 and 9.53 cm pipes. Recent measurements of Al-Sarkhi and Hanratty (2002) reveal that drop size increases with pipe diameter to the power of 0.5 for air and water flowing in horizontal pipes. A goal of this communication is to revisit the work of Pan and Hanratty (2002) by using this new information.

* Corresponding author. Tel.: +1-217-333-1318; fax: +1-217-333-5052.
E-mail address: hanratty@scs.uiuc.edu (T.J. Hanratty).

0301-9322/03/$ - see front matter
PII: S0301-9322(02)00126-X

Two mechanisms have been presented for the transition from stratified to annular flow in horizontal pipes: one suggests that wetting of the top wall of the pipe is initiated by large-amplitude waves which wrap around the pipe circumference. The other suggests that annular flow is caused by an entrainment-deposition mechanism. Lin and Hanratty (1987) carried out an extensive study on flow patterns and concluded that the transition in a 9.53 cm pipe occurs primarily through the deposition of droplets. This mechanism is dominant in a 2.54 cm pipe only for superficial liquid velocities smaller than 0.015 m/s. A second goal of this communication is to explore a definition of the transition from stratified to annular flow based on a calculated film thickness at the top of the pipe by using the droplet deposition mechanism.

2. Method of correlation

2.1. Concentration distribution

The concentration of drops is assumed to be approximately uniform in planes perpendicular to the direction of gravity; that is, it is only a function of the vertical axis, y. An integration of a mass balance equation gives the following equations (Paras and Karabelas, 1991; Pan and Hanratty, 2002) for situations in which the concentrations are small enough that particle–particle interactions can be ignored:

$$\varepsilon \frac{\mathrm{d}C}{\mathrm{d}y} + u_{\mathrm{T}} C = a(y) \tag{1}$$

$$a(y) \equiv -D \int \frac{R_{\mathrm{A}} - R_{\mathrm{D}}}{(D/2)^2 - y^2}\,\mathrm{d}y - B \tag{2}$$

where $\varepsilon = \zeta(D/2)u^*$ is the eddy diffusivity of the drops, ζ is a constant, D is the diameter of the pipe, u^* is the friction velocity, C is the concentration of droplets, u_{T} is the terminal velocity of droplets, R_{A} is the rate of atomization, R_{D} is the rate of deposition, B is an integration constant and y is the distance from the bottom of the pipe. The equation indicates that gravitational settling is opposed by turbulent diffusion. The third term, $a(y)$, represents a source or sink of drops.

The evaluation of $a(y)$ requires an accurate representation of the variation of the film thickness and of the rate of atomization around the pipe circumference. This is not available, so we have chosen to ignore this term, as did Pan and Hanratty (2002). The motivation for this is that analyses of the film distribution indicate that the exchange of liquid between the film and the core is having a small effect, except in a region close to the top of the pipe when disturbance waves do not wrap around the circumference (Laurinat et al., 1985). The integration of Eq. (1) then gives Eq. (3):

$$C = C_0 \exp\left(-\frac{u_{\mathrm{T}}}{\varepsilon} y\right) \tag{3}$$

where C_0 is the concentration of drops at the bottom of the pipe. If the relation for ε is substituted into Eq. (3) one obtains

$$C = C_0 \exp\left(-\frac{2u_T y}{\xi u^* D} \right) \tag{4}$$

The influence of pipe diameter enters through the scaling of the eddy diffusivity and through its effects on the dimensionless group in the exponential, u_T/u^*.

The particles are assumed to be spherical so that the terminal velocity is given as

$$u_T^2 = \frac{4dg\rho_L}{3C_D\rho_G} \tag{5}$$

where d is the drop diameter, g is the acceleration due to gravity and C_D is the drag coefficient. The recent study by Al-Sarkhi and Hanratty (2002) indicates that the volume median diameter of the drops, d_{50}, in an air–water flow can be approximated as

$$\left(\frac{d_{50} U_{SG}^2 \rho_G}{\sigma} \right)^{0.37} \left(\frac{d_{50}}{D} \right)^{0.36} = 0.196 \tag{6}$$

where U_{SG} is the superficial gas velocity, ρ_G is the density of the gas and σ is the surface tension. The distribution of drop sizes can be represented by a log-normal distribution function.

2.2. Film thickness at the top of the pipe

For the case in which annular flow is initiated by drop wetting, the transition will start with the creation of a stable film at the top of the pipe. The film would be laminar and covered with capillary ripples. Consider a coordinate system in which y is the distance from the wall and x is the distance from the top of the pipe in the circumferential direction. A force balance on the wall film gives

$$\frac{d\tau_{yx}}{dy} + \rho_L g \sin\theta = 0 \tag{7}$$

where $\tau_{yx} = \mu_L(du_x/dy)$ and θ is the angle measured from the top of the pipe. Eq. (7) can be integrated to obtain $u_x(y)$ by assuming $u_x = 0$ at $y = 0$ and that $\tau_{yx} = 0$ at $y = h$. This implies that the influence of secondary flows in the gas can be neglected and that the ripple waves are perpendicular to the x-axis. The local mass flow per unit length in the x-direction is given as

$$\Gamma_x = \int_0^h \rho_L u_x \, dy \tag{8}$$

As discussed by Laurinat et al. (1985), the change of Γ_x in the circumferential direction is obtained from a mass balance:

$$\frac{1}{a}\frac{d\Gamma_x}{d\theta} = R_D - R_A \tag{9}$$

where a is the pipe radius, R_D is the rate of deposition of drops per unit area and R_A is the rate of atomization per unit area. The rate of atomization at the top of the pipe would be zero at the initiation of annular flow by droplet deposition. The height of the film at the top of the pipe is then calculated as

$$h = \left(\frac{3R_D D v_L}{2g\rho_L} \right)^{1/3} \tag{10}$$

where v_L is the kinetic viscosity of the liquid.

3. Implementation

The local entrainment is determined by withdrawing samples through an impact tube. Thus, local values of droplet flux, F_{LE}, were measured. The calculation of the concentration is obtained from these measurements by using the equation:

$$C = \frac{F_{LE}}{SU_{local}} \tag{11}$$

where U_{local} is the local gas velocity and S is the ratio of the local drop velocity to the local gas velocity. Paras and Karabelas (1991) did not measure the velocity so they used a symmetric logarithmic velocity profile, typical of what would be found for roughened walls. Measurements by Williams et al. (1996) show that the velocity profile is highly asymmetric. To simplify the analysis, a plug flow is assumed and the velocity is taken as the superficial value, U_{SG}. Williams et al. (1996) calculated a mean slip ratio, S, by integrating the measured gas velocities for different values of S until the calculated volumetric gas flow was correct. In the calculations in this paper an average of the values obtained by Williams et al. was used, that is, $S = 0.7$.

A bulk mean concentration, $\langle C \rangle$, can be calculated from the measurements of entrainment. Thus

$$\langle C \rangle = \frac{EW_L}{Q_g S} \tag{12}$$

where E is the entrainment, Q_g is the volumetric gas flow and W_L is the liquid mass flow rate. The concentration, C_0, that appears in Eq. (4) can be related to $\langle C \rangle$ by integrating over the cross section, assuming a plug flow:

$$\langle C \rangle = \frac{1}{A} \int C_0 \exp\left(-\frac{u_T}{\varepsilon} y \right) \mathrm{d}A \tag{13}$$

where $\mathrm{d}A = S(y)\mathrm{d}y$ and S is the chord at y. As shown by Pan and Hanratty Eq. (13) can be easily modified to take account of a distribution of drop sizes. Again, for simplicity, the drops were assumed to have a single size, that is, $d = d_{50}$.

The final equation that was tested is Eq. (4), where u_T is calculated with Eq. (5) and $d = d_{50}$ is obtained from Eq. (6). The friction velocity is calculated from the measured pressure gradient, and C_0 is obtained from Eq. (13). Considering the number of approximations that are made, the final method used to represent the concentration profile may be considered to be obtained from dimensional analysis for which

$$\frac{C}{\langle C \rangle} = f\left(\frac{y}{D}, \frac{u_T}{u^*} \right). \tag{14}$$

The rate of deposition was calculated as the product of the calculated concentration of drops at the top wall, C_w, and the average velocity of the drops moving toward the wall, $V_{average}$, that is, the deposition velocity:

$$R_D = C_w V_{average}. \tag{15}$$

The approach used by Pan and Hanratty (2002) was used to calculate $V_{average}$. The distribution of drop velocities is assumed to be described by a Gaussian function with a mean of $-u_T$ and a standard deviation of σ_p. The standard deviation, σ_p, is related to the standard deviation of the fluid velocity fluctuations by the method described by Pan and Hanratty (2002).

4. Results

4.1. Concentration profiles

Values of C/C_0 are plotted against y/D in Fig. 1 for the measurements of F_{LE} obtained by Williams et al., where $\langle C \rangle$ is calculated from Eq. (12) and C_0 from Eq. (13). The parameter is gas velocity. Decreases in U_{SG} correspond to increases in u_T/u^* because of the increase in d_{50} and the decrease in u^*. The measurements are seen to be very sensitive to changes in U_{SG}.

Measurements by Paras and Karabelas are presented in Fig. 2. In these experiments U_{SL} was varied. An increase in U_{SL} gives rise to an increase in the interfacial friction factor. Therefore, u_T/u^* will decrease with increasing U_{SL} if U_{SG} is kept constant. Both the experiments of Williams et al. (1996) and of Paras and Karabelas (1991) show decreases in C/C_0 with increases in u_T/u^*.

The lines in Figs. 1 and 2 represent Eq. (4) with $\zeta = 0.165$. They present a rough fit to the data, considering that secondary flows in the gas (Dykhno et al., 1994) are not taken into account. Pan

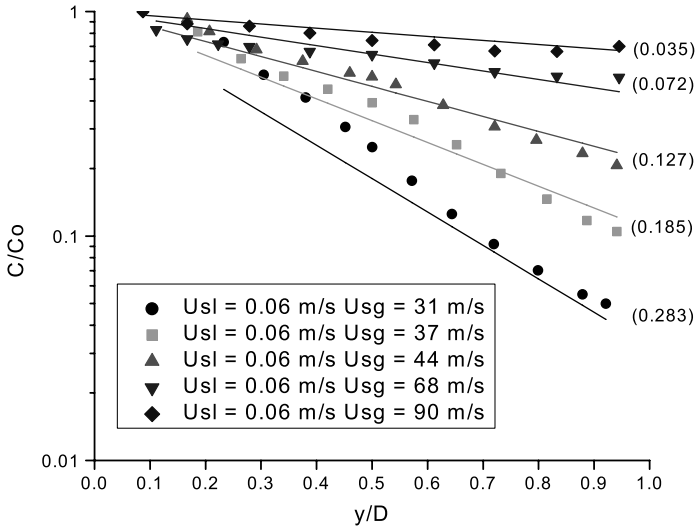

Fig. 1. Comparison of measurements of droplet concentrations with Eq. (4) for air–water flows in a 9.53 cm pipe. The values of u_T/u^* are shown in parentheses.

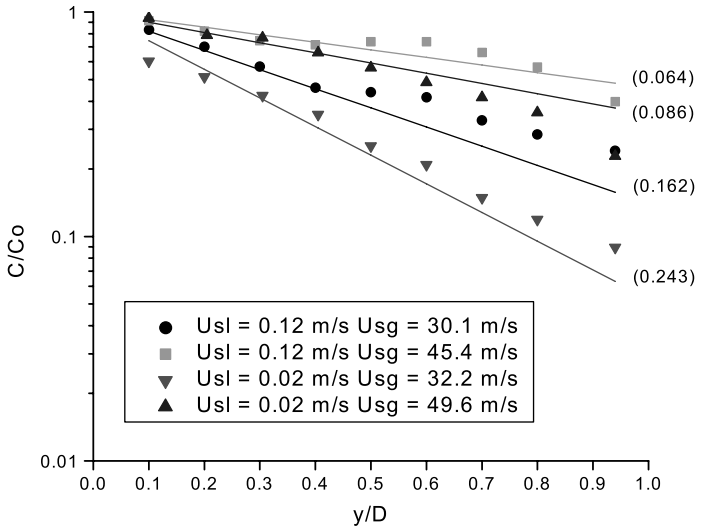

Fig. 2. Comparison of measurements of droplet concentrations with Eq. (4) for air–water flows in a 5.08 cm pipe. The values of u_T/u^* are shown in parentheses.

and Hanratty (2002) employed a similar approach but had to use different values of the parameter in Eq. (4) to fit the experimental data, $\xi = 0.04$ for the 9.53 cm pipe and $\xi = 0.08$ for the 5.08 cm pipe. The calculated C/C_0 is very sensitive to the choice of ξ. For example, the calculated value of C/C_0 at the top of the pipe would increase by a factor of about 10 if $\xi = 0.08$ were used by Pan and Hanratty for the 9.53 cm pipe. The inclusion of an effect of pipe diameter on the drop size, therefore, provides an improvement in the correlation.

4.2. Film thickness at transition for air–water flow

Film thicknesses, calculated with Eq. (10) for air and water flowing in a horizontal pipe, are presented in Fig. 3. The numbers in the parentheses are the drop sizes in microns. Measurements of film thickness at the top of the pipe, obtained by Williams et al. (1996), are also presented in Fig. 3. These were obtained by a conductance technique, which could not make measurements below 60 μm. The agreement between the measurements and the calculations is satisfactory. Decreases in the drop size cause increases in the concentration of drops close to the top wall and increases in R_D. Thus the film thickness at the top wall is very sensitive to drop size.

The transition to annular flow for $U_{SL} = 0.06$ m/s, suggested by Lin and Hanratty (1987), is indicated by an arrow in Fig. 3. This suggests that a continuous stable film at the top wall is realized when $h \cong 20$ μm. Andreussi et al. (1985) observed that disturbance waves (or a transition to turbulence) occurs at a film Reynolds number, in the mean flow direction, of about 380. Local Reynolds numbers can be calculated by a method described by Asali et al. (1985). This transition is indicated by a second arrow in Fig. 3.

Fig. 4 shows transitions from stratified to annular flow, defined by Lin and Hanratty (1987), for conditions where the change is controlled by droplets wetting the top wall. The transition for a 2.53 cm Plexiglas pipe is indicated by the dotted curve. The transition for a 9.53 cm Plexiglas pipe

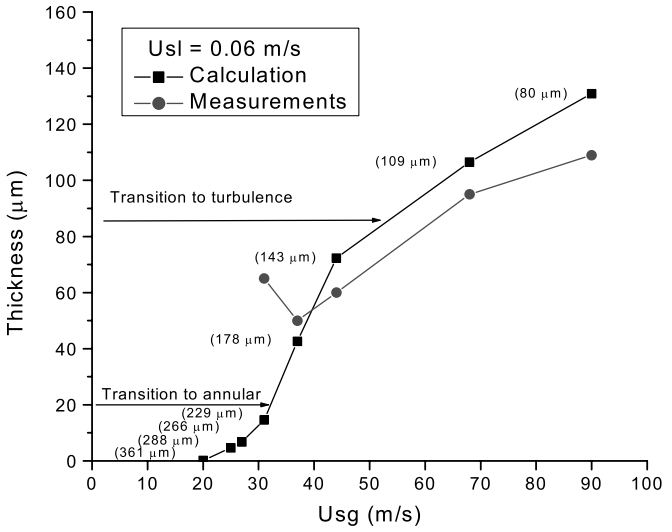

Fig. 3. Comparison of measurements of film thickness at the top wall with Eq. (10) for air–water flows in a 9.53 cm pipe. Drop sizes are shown in parentheses.

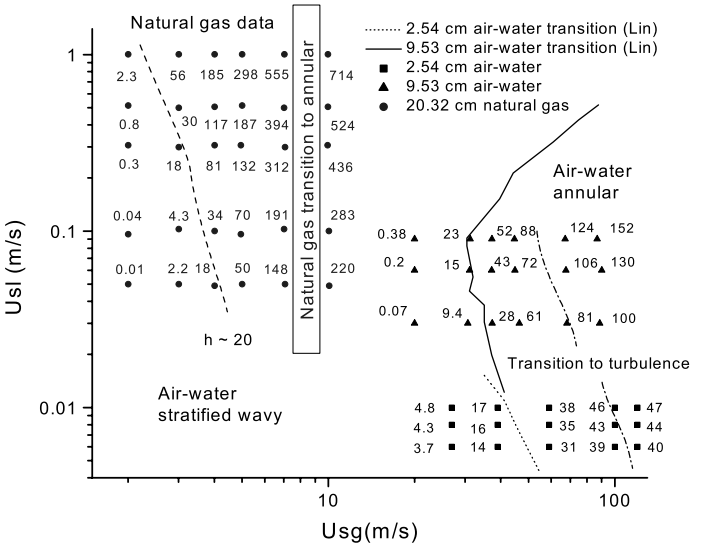

Fig. 4. Transition from stratified to annular flow. Calculated film thicknesses at the top wall using Eq. (10) are shown in micrometers.

is indicated by the solid curve. Calculated film thicknesses at the top of the pipe for the different flow conditions considered by Lin and Hanratty are given. An average film thickness at transition of about 20 μm is obtained for the 9.53 and 2.54 cm pipes. The transition to turbulence is also indicated by the dash-dot curve.

4.3. Transition in a natural gas pipeline

Data for the transition to an annular flow in a 20.32 cm natural gas pipeline are shown in the left side of Fig. 4 (Zabaras, 2002). The operating conditions are quite different from what exists for air–water flow. The gas density is 65 kg/m^3; the pressure is 75 bars; the liquid density is 720 kg/m^3; the surface tension is 0.0118 N/m; the liquid viscosity is 0.00055 mPa s; the gas viscosity is 1×10^{-5} mPa s. The pipeline was constructed of steel that had an equivalent sand roughness of 100–150 μm.

Film thicknesses at the top wall were calculated for conditions for which pressure drops were available. These are indicated under the dots in Fig. 4. A value of $h \cong 20$ μm is indicated by the dashed curve. Critical U_{SG} of 2–4 m/s are calculated if $h \cong 20$ μm is assumed to be the critical film thickness. These are lower than the measured critical U_{SG} of 7–10 m/s. A possible explanation is that the pipe roughnesses are larger than the calculated critical film thickness (for a smooth wall).

5. Discussion

5.1. Prediction of drop concentration profile

Measurements of droplet concentration profiles for air and water flowing in horizontal pipes with diameters of 5.08 and 9.53 cm are analyzed in this paper. Eq. (4) with $\zeta = 0.165$ provides a good approximation of the data. From Eq. (13) one sees that concentration C_0 is a function of u_T/u^* and $\langle C \rangle$. The data show that $C/\langle C \rangle = f(y/D, u_T/u^*)$. For a given y/D, the concentration C/C_o is found to decrease with increasing u_T/u^*. This dependency is displayed by experiments in which U_{SL} is kept constant and U_{SG} is increased. Then u_T/u^* decreases because drop size decreases with increasing U_{SG}. It is also displayed in experiments where U_{SG} is kept approximately constant and U_{SL} increases. In this case u_T/u^* decreases because u* increases. A main point that is made in this paper is that the influence of pipe diameter on drop size needs to be taken into account. Larger drop sizes lead to larger u_T and, therefore, greater asymmetry of the concentration profile.

Clearly, there are differences between the measurements and Eq. (4). There is room for improvement both in the theory and in the measurements. A correlation that includes the influence of the $a(y)$ term in Eq. (1) could introduce new dimensionless groups. A possible improvement in the correlation can be obtained by abandoning the assumption of a plug flow, so that C is defined using the local velocity, rather than U_{SG}. This is a difficult task because the gas velocity profile is a complicated function which is not presently available. Some justification for using the simplified approach can be obtained from the study in a 9.53 cm pipe. Williams et al. (1996) measured the velocity profiles for some of the runs in which droplet fluxes were measured, so that concentration profiles could be calculated with local gas velocities. The results obtained in this way were not appreciably different from those obtained by using a plug flow assumption.

5.2. Transition to annular flow

Eq. (10) was derived to describe the film height at the top of the pipe. It assumes that the flow is laminar, that $R_A = 0$ and that the stresses at the interface do not have a circumferential com-

ponent. It is noted that there is a direct dependence on pipe diameter because drainage is smaller in larger pipes. Since R_D depends on the concentration of drops at the top wall and on $V_{average}$, the height of the film at the top of the pipe, h, decreases with increasing drop size. A comparison of calculated and measured h in a 9.53 cm pipe provides support for using this approach to predict the transition to annular flow when droplet deposition is the controlling mechanism.

High speed motion pictures reveal that atomization occurs by the removal of small wavelets which exist in flow surges in the liquid film (Woodmansee and Hanratty, 1969). These results have prompted the suggestion that atomization occurs through an inviscid Kelvin–Helmholtz instability, which pictures two fluids flowing parallel to one another with uniform velocity profiles. A critical relative velocity of about 6.6 m/s is predicted for air–water at atmospheric pressure. Andritsos and Hanratty (1987) found that a KH instability leads to the formation of large amplitude irregular waves, that drop formation could be detected at a gas velocity which is twice as large as needed for a KH instability, and that transition to annular flow occurs at velocities 2–3 times larger than that needed to initiate atomization. For a natural gas pipe line with a diameter of 20.32 cm, a KH instability occurs at about 0.54 m/s. However, the transition to annular flow for a natural gas pipe line is found to occur at 7–10 m/s by using visual observations.

These results indicate that it could be undesirable to link transition to annular flow to a KH instability when droplet wetting is the controlling mechanism. Therefore, the mechanism that turbulent mixing in the gas flow must be sufficient to create a stable film at the top wall was pursued. A comparison with the observations in 2.54 and 9.53 cm pipes by Lin and Hanratty (1987) indicates that transition occurs in a Plexiglas pipe at a film thickness of about 20 μm.

Values of a non-dimensional film thickness at transition, h^+, were also calculated by using the method described by Asali et al. (1985). This is found to be approximately equal to 2. The expectation is that this result could depend on the wetting properties of the surface. Tatterson (1975) found that the wetting and the formation of a continuous film in an air–water flow is enhanced by roughing a Plexiglas surface with sandpaper. Further improvements in forming a film were realized by painting the roughened surface with a colloid of hydrous tin oxide. On the other hand, measurements of Hobler and Czajka (1968) show only modest effects of different surface materials on the dimensionless critical film thickness (Mikielewicz and Moszynski, 1976) for the breakup of a freely-falling film.

Observations of the transition indicate that droplets impinge on the top wall where they coalesce to form larger drops. These coalesce to form rivulets which, at large enough flows, spread out to create a continuous film. There is a similarity between this process and the process of dryout which has received so much attention in the heat transfer community.

Therefore, it is of interest to discuss two studies carried out by Hewitt and Lacey (1965) for air flowing over a water film that was moving upward over an acrylic wall under conditions that atomization was not occurring. In one of these it was found that the water film forms dry spots for h^+ values of about 1.5–2.7. In the second, a dry spot was created by blowing air at an upward flowing annular film. If the flow of the film was large enough, the dry spot disappeared. In this way, a critical h^+ between 4.62 and 6.87 was determined. These results are to be compared with the critical $h^+ \cong 2$ that we estimated from the experiments of Lin and Hanratty (1987) on the transition to annular flow. We also should point out that Asali et al. (1985) observed h^+ as low as about 2 for water–glycerine solutions flowing in vertical gas–liquid annular flows under conditions that atomization was not occurring.

The calculations for a natural gas pipeline were of particular interest because of the very wide difference between the critical U_{SG} for a KH instability and the U_{SG} at which a transition to annular flow is observed. The calculations indicate that the transition occurs for much thicker films than those calculated (and observed) for the air–water flow. One possible explanation is that the correlation used to predict drop size is not applicable. A different mechanism could be operable so that drop sizes are larger than predicted. However, a more likely explanation is the use of different pipe materials. The pipe had a roughness size which was of the order of 100–150 μm. (This is much larger than what would be obtained by roughening a Plexiglas surface with sandpaper.) If the criterion for transition is that the liquid must flood these roughnesses, then film thickness much larger than 20 μm would be needed.

Acknowledgement

This work was supported by the Engineering Research Program of the Office of Basic Energy Sciences at the Department of Energy under grant DOE DEF G02-85ER-13556.

References

Al-Sarkhi, A., Hanratty, T.J., 2002. Effect of pipe diameter on the drop size in a horizontal annular gas–liquid flow. Int. J. Multiphase Flow 28, 1617–1629.

Andreussi, P., Asali, J.C., Hanratty, T.J., 1985. Initiation of roll waves in gas–liquid flows. AIChE J. 31, 119–126.

Andritsos, N., Hanratty, T.J., 1987. Interfacial instabilities for horizontal gas–liquid flows in pipelines. Int. J. Multiphase Flow 13, 583–603.

Asali, J.C., Hanratty, T.J., Andreussi, P., 1985. Interfacial drag and film height for vertical annular flow. AICHE J. 31, 895–902.

Dykhno, L.A., Williams, L.R., Hanratty, T.J., 1994. Maps of mean gas velocity for stratified flows with and without atomization. Int. J. Multiphase Flow 20, 691–702.

Hewitt, G.F., Lacey, P.M.C., 1965. The breakdown of the liquid film in annular two-phase flow. Int. J. Heat Mass Transfer 8, 781–791.

Hobler, T., Czajka, J., 1968. Minimal wetting of a flat surface. Chemia Stosow 2B, 169 (in Polish).

Laurinat, J.E., Hanratty, T.J., Jepson, W.P., 1985. Film thickness distribution for gas–liquid annular flow in a horizontal pipe. PCH PhysicoChemical Hydrodynamics 6, 179–195.

Lin, P.Y., Hanratty, T.J., 1987. Effect of pipe diameter on flow patterns for air–water flow in horizontal pipes. Int. J. Multiphase Flow 13, 549–563.

Mikielewicz, J., Moszynski, J.R., 1976. Minimum thickness of a liquid film flowing vertically down a sold surface. Int. J. Heat Mass Transfer 19, 771–776.

Pan, L., Hanratty, T.J., 2002. Correlation of entrainment for annular flow in horizontal pipes. Int. J. Multiphase Flow 28, 385–408.

Paras, S.V., Karabelas, A.L., 1991. Droplet entrainment and deposition in horizontal annular flow. Int. J. Multiphase Flow 17, 455–468.

Tatterson, D.F., 1975. Rates of atomization and drop size in annular two-phase flow. Ph.D. Thesis, University of Illinois, Urbana.

Williams, L.R., Dykhno, L.A., Hanratty, T.J., 1996. Droplet flux distributions and entrainment in horizontal gas–liquid flows. Int. J. Multiphase Flow 22, 1–18.

Woodmansee, D.E., Hanratty, T.J., 1969. Mechanism for the removal of droplets from a liquid surface by a parallel air flow. Chem. Eng. Sci. 24, 299–307.

Zabaras, G., 2002. Private communication.